Interleukin-6 and chondrocyte mineralisation act in tandem to promote experimental osteoarthritis

Sonia Nasi,[1] Alexander So,[1] Christèle Combes,[2] Michel Daudon,[3] Nathalie Busso[1]

[1]Service of Rheumatology, Department of Musculoskeletal Medicine, CHUV and University of Lausanne, Lausanne, Switzerland
[2]CIRIMAT, UMR 5085 INPT-UPS-CNRS, Université de Toulouse, ENSIACET, Toulouse, France
[3]AP-HP, service d'Explorations Fonctionnelles, hôpital Tenon, Paris, France

ABSTRACT

Objectives Basic calcium phosphate (BCP) crystal and interleukin 6 (IL-6) have been implicated in osteoarthritis (OA). We hypothesise that these two factors may be linked in a reciprocal amplification loop which leads to OA.

Methods Primary murine chondrocytes and human cartilage explants were incubated with hydroxyapatite (HA) crystals, a form of BCP, and the modulation of cytokines and matrix-degrading enzymes assayed. The ability of IL-6 to stimulate chondrocyte calcification was assessed in vitro. The mechanisms underlying the effects of HA on chondrocytes were investigated using chemical inhibitors, and the pathways mediating IL-6-induced calcification characterised by quantifying the expression of genes involved in chondrocyte mineralisation. The role of calcification in vivo was studied in the meniscectomy model of murine OA (MNX), and the link between IL-6 and cartilage degradation investigated by histology.

Results In chondrocytes, BCP crystals stimulated IL-6 secretion, further amplified in an autocrine loop, through signalling pathways involving Syk and PI3 kinases, Jak2 and Stat3 molecules. Exogenous IL-6 promoted calcium-containing crystal formation and upregulation of genes involved in calcification: the pyrophosphate channel Ank, the calcium channel Annexin5 and the sodium/phosphate cotransporter Pit-1. Treatment of chondrocytes with IL-6 inhibitors significantly inhibited IL-6-induced crystal formation. In meniscectomised mice, increasing deposits of BCP crystals were observed around the joint and correlated with cartilage degradation and IL-6 expression. Finally, BCP crystals induced proteoglycan loss and IL-6 expression in human cartilage explants, which were reduced by an IL-6 inhibitor.

Conclusions BCP crystals and IL-6 form a positive feedback loop leading to OA. Targeting calcium-containing crystal formation and/or IL-6 are promising therapeutic strategies in OA.

INTRODUCTION

Osteoarthritis (OA) is the most common form of chronic arthropathy and a leading cause of pain and disability. Biomechanical factors, joint trauma, age, gender and obesity have been identified as risk factors for OA development. OA is characterised by cartilage degradation, subchondral bone changes and mild synovitis. Although OA is not considered an inflammatory disease, several cytokines have catabolic effects on cartilage matrix.[1] However, it remains unclear if there is a common link that unites mechanical and inflammatory mechanisms in OA pathogenesis.

A common denominator that potentially integrates these mechanisms could be articular calcium-containing crystals. Crystal deposits were identified in 50% of synovial fluids[2] and in 100% of cartilage obtained during joint replacement[3] and correlated with the severity of radiographic and histological OA.[4] Calcium crystals were also found in some normal joints[5 6] suggesting that calcifications are present before cartilage breakdown. Pathogenic crystals encompass calcium pyrophosphate dihydrate (CPPD) and basic calcium phosphate (BCP) crystals, (the latter including octacalcium phosphate (OCP), carbonated-apatite (CA) and hydroxyapatite (HA) crystals),[7] and are generated by mineralising-competent cells and their cell membrane-derived matrix vesicles. In particular, high extracellular inorganic pyrophosphate (PPi) and inorganic phosphate (Pi) lead to CPPD and BCP crystal formation, respectively.[8] The pathways which regulate this balance involve multiple ectoenzymes (Pc-1 that cleaves ATP in AMP and PPi, and Tnap that hydrolyses PPi in Pi) and transporters such as the PPi transporter Ank and the Pi transporters Pit-1 and Pit-2, and the Ca^{2+} transporter AnnexinV.[9] Loss of function mutations in Pc-1 or Ank led to HA crystal deposition, calcifications and to OA-like changes in murine joints,[10–12] and cartilage of patients with OA showed increased expression of Pc-1 and Ank.[8 13] We demonstrated that intra-articular injection of BCP crystals in mice led to low grade inflammation and cartilage degradation.[14] It has been reported that CPPD and BCP crystals can activate cells via different signalling pathways.[15–21] In chondrocytes, it has been reported that BCP crystals induce inducible nitric oxide (iNOS) expression, nitric oxide (NO) production [20] and Mmp-13 production,[22] but whether crystals induce additional inflammatory and catabolic response in this cell type, and the possible underlying signalling pathways, remains to be explored.

IL-6 is a pleiotropic cytokine increased in synovial fluids and sera of patients with OA, and increased IL-6 serum level correlates with radiographic knee OA.[23] IL-6 induced Mmp-1, Mmp-3 and Mmp-13 production by chondrocytes and synoviocytes.[24 25] The catabolic effects of injury together with tumour necrosis factor-alpha (TNF-α) on cartilage were mediated by endogenous IL-6.[26] Using in vitro and in vivo approaches, Ryu *et al*[27] demonstrated that IL-6 was a crucial mediator of hypoxia inducible factor-2-alpha (HIF-2α)-induced cartilage destruction via upregulation of Mmp-3 and Mmp-13 and found that IL-6

deficient mice were protected against OA. Although these studies support a key role of IL-6 in OA, further investigations are needed to clarify the triggers of IL-6 within the joint and IL-6 effects on chondrocytes.

In the present study we evaluated the effects of BCP crystals in primary murine chondrocytes, in the meniscectomy model of murine OA and in human cartilage explants. We demonstrated that BCP crystals trigger IL-6 secretion and IL-6-mediated cartilage degradation. Furthermore, we investigated the possible signalling pathway involved in BCP-induced IL-6 secretion in chondrocytes. Finally, we studied the mechanism by which IL-6 could be of a key importance in chondrocyte mineralisation. Our experimental data provide: (1) novel insights in the mechanisms of OA, suggesting interplay between BCP crystals and IL-6 and (2) novel therapeutic targets for this frequent and as yet poorly treated chronic condition.

METHODS

Mice and induction of experimental OA

Female C57BL/6 mice (8–10 weeks old) were purchased from Charles River. Mice were anaesthetised and knee joint instability was induced surgically by partial medial meniscectomy (MNX) of the right knee, whereas the contralateral knee was sham-operated as control.[28] Experiments were performed in accordance with the Swiss Federal Regulations. The protocol was approved by the "Service de la consommation et des affaires vétérinaires du Canton de Vaud", Switzerland.

MicroCT scan

MicroCT scans were performed with a SkyScan 1076 X-ray μCT scanning system (SkyScan, Belgium) using the following parameters: 18 μm resolution, 60 kV, 167 μA, 0.4° rotation step over 360°, 0.5 mm aluminum filter, 1180 ms exposure time. In vivo or ex vivo acquisitions were made using anaesthetised mice or formol-fixed knees, respectively. Images were reconstructed using NRecon V.1.6.6.0 (Skyscan, Belgium) considering the following parameters: grey values=0.0000–0.105867, ring artefact reduction=3, beam hardening correction=40%. Quantitative analyses (bone mineral density (g/cm^3), new formation volume (mm^3) and new formation crystal content (μg)) were performed using CTAnalyzer V.1.10 (SkyScan, Belgium) for different volumes of interest.

Mouse knee histology and immunohistochemistry

Knee joints were processed and histological analysis performed as described.[29] Immunohistochemical analysis of collagen 2, Mmp-induced neoepitope VDIPEN and IL-6 was performed using an anticollagen 2 biotinylated monoclonal antibody (MD Bioproduct), an affinity-purified anti-Val-Asp-Iso-Pro-Glu-Asn metalloproteinase generated neoepitope (VDIPEN) antibody[30] and an anti IL-6 antibody (Abcam), respectively. IL-6 scoring was performed in the anteromedial part of the knee joint (following the same method as for Safranin-O score).

Calcium phosphate crystals

BCP and CPPD crystals were synthesised as previously published.[31] BCP crystals were sterilised by γ-radiation and assessed as pyrogen-free. Prior to experimentation, crystals were resuspended in sterile phosphate buffered saline (PBS) and sonicated for 5 min.

Articular chondrocyte preparation

Chondrocytes were generated from C57BL/6J mice as described previously.[32] Cells (3.5×10^4 cells/cm^2) were cultured for 7 days in complete Dulbecco's modified Eagle Medium (DMEM) (10% fetal bovine serum (FBS)). Chondrocyte stimulations with crystals were performed in serum-free DMEM. For chondrocyte mineralisation analysis, cells were cultured for 3 days in complete Fitton-Jackson Modified (BJGb) medium (Gibco) (10% FBS, 50 μg/mL ascorbic acid, 20 mM β-glycerol phosphate), stimulated or not with 10 ng/mL of IL-6 (Gibco PMC0064) and treated or not with different inhibitors: Syk kinase inhibitor piceatannol (100 μM, Calbiochem 527948), PI3 kinase inhibitor Wortmannin (20 μM, Sigma W1628), anti-IL-6 receptor (8 μg/mL, R&D System AF1830) or Jak2 inhibitor AG490 (50 μM, Calbiochem 658401). Medium was changed for the last 4 days.

Fourier transform infrared spectroscopy analysis

Fourier transform infrared spectroscopy (FTIR) was used for in vitro (chondrocytes) and in vivo (dissected ectopic calcifications in knee joints) analyses. The mineral phase was evaluated by FTIR Bruker Vector 22 (BruckerSpectrospin, Wissembourg), as previously described.[33 34]

Crystal detection from chondrocyte cultures

Articular chondrocytes cultured for 7 days were washed in PBS and crystal deposition analysed as previously described.[35]

Calcium phosphate crystal stimulation

Chondrocytes were primed overnight with100 ng/mL Pam3Cys, where indicated, and stimulated with BCP or CPPD crystals or

Table 1 qRT-PCR analysis

Gene	Forward primer (5′→3′)	Reverse primer (5′→3′)
Adamts-4	GCC CGA GTC CCA TTT CCC GC	GCC ATA ACC GTC AGC AGG TAG CG
Adamts-5	GAC AGA CCT ACG ATG CCA CCC AGC	ATG AGC GAG AAC ACT GAC CCC AGG
Ank	TGT CAA CCT CTT CGT GTC CC	GAC AAA ACA GAG CGT CAG CG
Coll2	ACA CTT TCC AAC CGC AGT CA	GGG AGG ACG GTT GGG TAT CA
Coll10	AAA CGC CCA CAG GCA TAA AG	CAA CCC TGG CTC TCC TTG G
Anx5	CCT CAC GAC TCT ACG ATG CC	AGC CTG GAA CAA TGC CTG AG
Gapdh	CTC ATG ACC ACA GTC CAT GC	CAC ATT GGG GGT AGG AAC AC
Il-1a	AAA CAC TAT CTC AGC ACC ACT TG	GGT CGG TCT CAC TAC CTG TG
Il-1b	CCA CCA ACA AGT GAT ATT CTC CAT G	GTG CGG TCT TTC ATT ACA CAG
Il-6	TCC AGT TGC CTT CTT GGG AC	GTG TAA TTA AGC CTC CGA CT
Tnf-a	CAT CTT CTC AAA ATT CGA GTG ACA A	TGG GAG TAG ACA AGG TAC AAC CC
Mmp-3	ATA CGA GGG CAC GAG GAG	AGA AGT AGA GAA ACC CAA ATG CT
Mmp-13	GCA GTT CCA AAG GCT ACA AC	GTC GGG TCA CAC TTC TCT G
Pc-1	CTG GTT TTG TCA GTA TGT GTG CT	CTC ACC GCA CCT GAA TTT GTT
Pit-1	CTC TCC GCT GCT TTC TGG TA	AGA GGT TGA TTC CGA TTG TGC
Pit-2	AAA CGC TAA TGG CTG GGG AA	AAC CAG GAG GCG ACA ATC TT
Runx2	GGG AAC CAA GAA GGC ACA GA	TGG AGT GGA TGG ATG GGG AT
Sox9	AAG ACT CTG GGC AAG CTC TGG A	TTG TCC GTT CTT CAC CGA CTT CCT
Tbp	CTT GAA ATC ATC CCT GCG AG	CGC TTT CAT TAA ATT CTT GAT GGT C
Tnap	TTG TGC CAG AGA AAG AGA GAG	GTT TCA GGG CAT TTT TCA AGG T

with 10 ng/mL IL-6. In some experiments, cells were treated with: piceatannol (100 μM), Wortmannin (20 μM), anti-IL-6 receptor (8 μg/mL), AG490 (50 μM) or cucurbitacin (10 μM, Calbiochem 238590). Supernatants were collected for cytokine ELISAs, and cells placed in TRIZOL for qRT-PCR analysis.

RNA was extracted and qRT-PCR with gene specific primers (table 1) was performed as previously described.[14]

Human cartilage explants experiments

Macroscopically intact knee cartilage from four patients with OA (Kellgren-Lawrence score of 4, mean age 73±10 years) was obtained from the Orthopedics Department (CHUV, Lausanne, Switzerland) at the time of joint replacement, with the approval of the hospital ethical committee and patients' written informed consent. Cartilage disks 6 mm diameter (9–20 disks/patient) were divided in halves, and each half was stimulated for 24 h in DMEM supplemented with 20 μg/mL ascorbic acid. Explants were stimulated with 500 μg/mL HA crystals in presence or absence of 5 μg/mL Actemra (tocilizumab, Roche) or Ilaris (canakinumab, Novartis). Supernatants were collected for ELISAs. Proteoglycans were examined by histology in formol-fixed Safranin-O-stained cartilage sections (0=normal to 4=completely degraded cartilage). IL-6 analysis (% of IL-6 positive cells out of three independent fields) was performed by immunohistochemistry using an anti-IL-6 antibody (US Biological Life Sciences).

Cytokine quantification

Supernatants were assayed using murine or human IL-6, TNF-α, IL-1β and monocyte chemoattractant protein-1 (MCP-1) ELISA

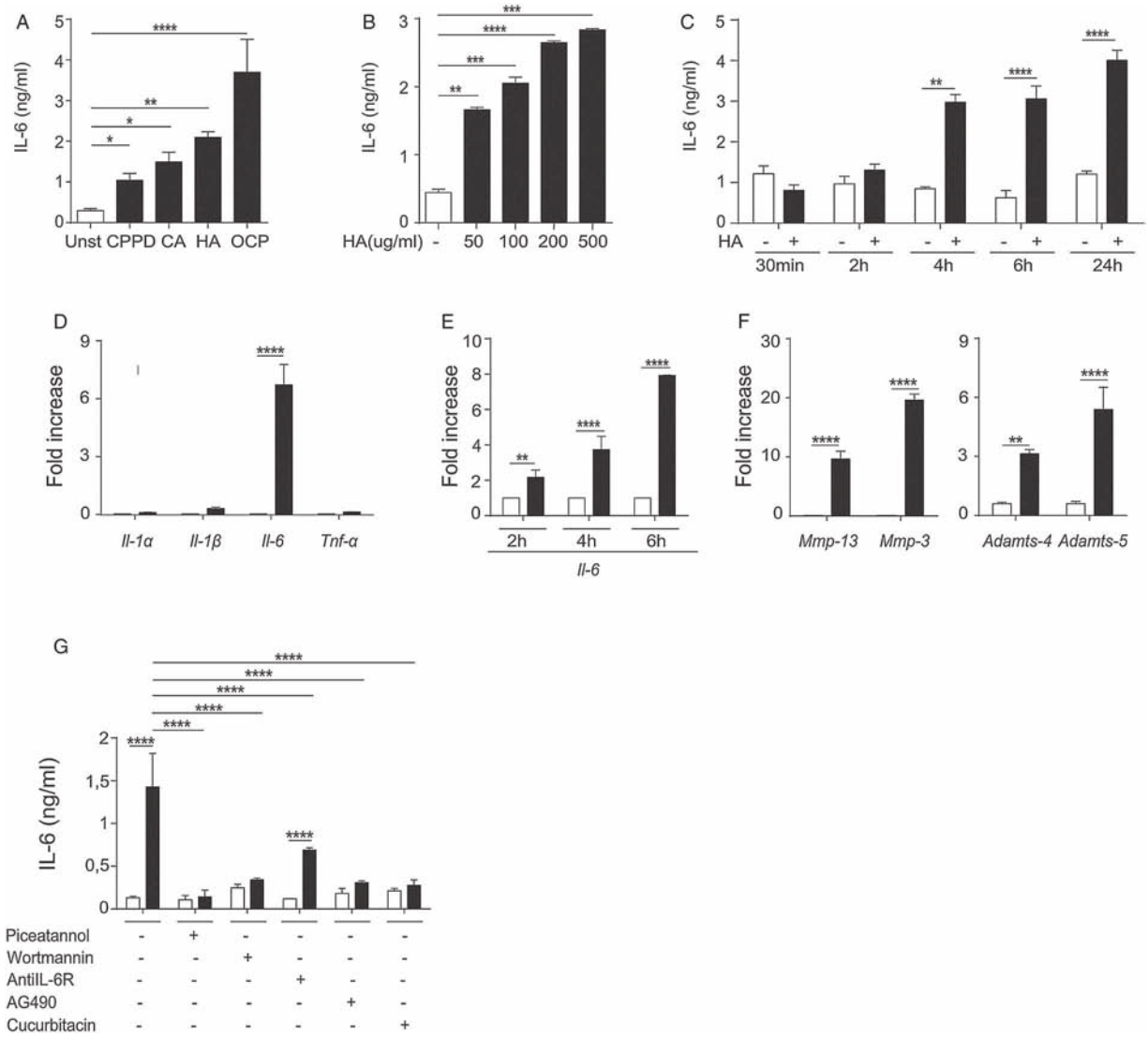

Figure 1 Basic calcium phosphate (BCP) crystals trigger proinflammatory and catabolic responses in murine chondrocytes. (A–C) IL-6 secretion by primed murine chondrocytes stimulated or not (A) with calcium pyrophosphate dihydrate and different BCP crystals for 6 h or (B) with different doses of hydroxyapatite (HA) crystals for 6 h or (C) with HA crystals at different time points. Values represent means±SD of triplicates from one representative experiment (D–F) qRT-PCR analysis of the indicated genes in not primed murine chondrocytes stimulated (black bars) with HA crystals or not (white bars) for 4 h (D), different time points (E) or 30 min (F). Results are expressed as the fold increase of gene expression in HA crystals treated over unstimulated chondrocytes, using the mean±SD of triplicate samples. (G) IL-6 secretion by primed murine articular chondrocytes stimulated (black bars) or not (white bars) with HA crystals and treated or not with piceatannol (100 μM), Wortmannin (20 μM), anti-IL6R (8 μg/mL), AG490 (50 μM) and cucurbitacin (10 μM) for 6 h. Values represent means±SD of triplicates from one representative experiment. *p<0.05, **p<0.01, ***p<0.001, ****p<0.0001.

kits (eBioscience) following the manufacturer's protocol. Results were read at 450 nm using the Spectrax M5e (Molecular devices).

Statistical analysis

All experiments were performed with triplicates and reproduced independently at least twice. Statistical analysis was performed using the Student's t test, one-way or two-way analysis of variance (ANOVA) test corrected with post hoc tests for multiple comparisons, or linear regression, where appropriate. Data was analysed with GraphPad Prism software (GraphPad, San Diego, California, USA).

RESULTS

BCP crystals induce IL-6 secretion by primary murine chondrocytes through Syk kinase, PI3 kinase, Jak2 and Stat3 signalling

Murine chondrocytes exposed to CPPD crystals and BCP crystals (CA, HA and OCP) secreted high amounts of IL-6 (figure 1A), while IL-1β and TNF-α remained undetectable. HA-induced IL-6 secretion was dose-dependent (figure 1B) and time-dependent (figure 1C). In line with the ELISA results, qRT-PCR analysis revealed significantly increased *IL-6* gene expression (6× compared with control) in HA-stimulated chondrocytes, whereas *IL-1α*, *IL-1β* and *TNF-α* expression was not modulated (figure 1D). IL-6 gene expression was modulated in a time-dependent manner (figure 1E). Additionally, the expression of the catabolic genes *Mmp-13* and *Mmp-3* and of *Adamts-4* and *Adamts-5* was strongly upregulated upon HA stimulation (figure 1F). Finally, HA-induced IL-6 secretion was abrogated by piceatannol and Wortmannin (figure 1G), both having no cytotoxic effects (results not shown). In addition, HA-induced IL-6 secretion was significantly diminished by a blocking IL-6 receptor antibody (anti-IL-6R) but not by an isotype matched control antibody (figure 1G and result not shown). Consistent with this latter result, AG490 and cucurbitacin also inhibited HA-induced IL-6 secretion (figure 1G).

HA crystals induce matrix degradation in human cartilage explants by IL-6 dependent mechanisms

Since BCP crystals led to massive secretion of IL-6 by murine articular chondrocytes and enhanced IL-6 expression in the meniscectomy model (see online supplementary figure S2), we investigated the role of HA-induced IL-6 in human cartilage

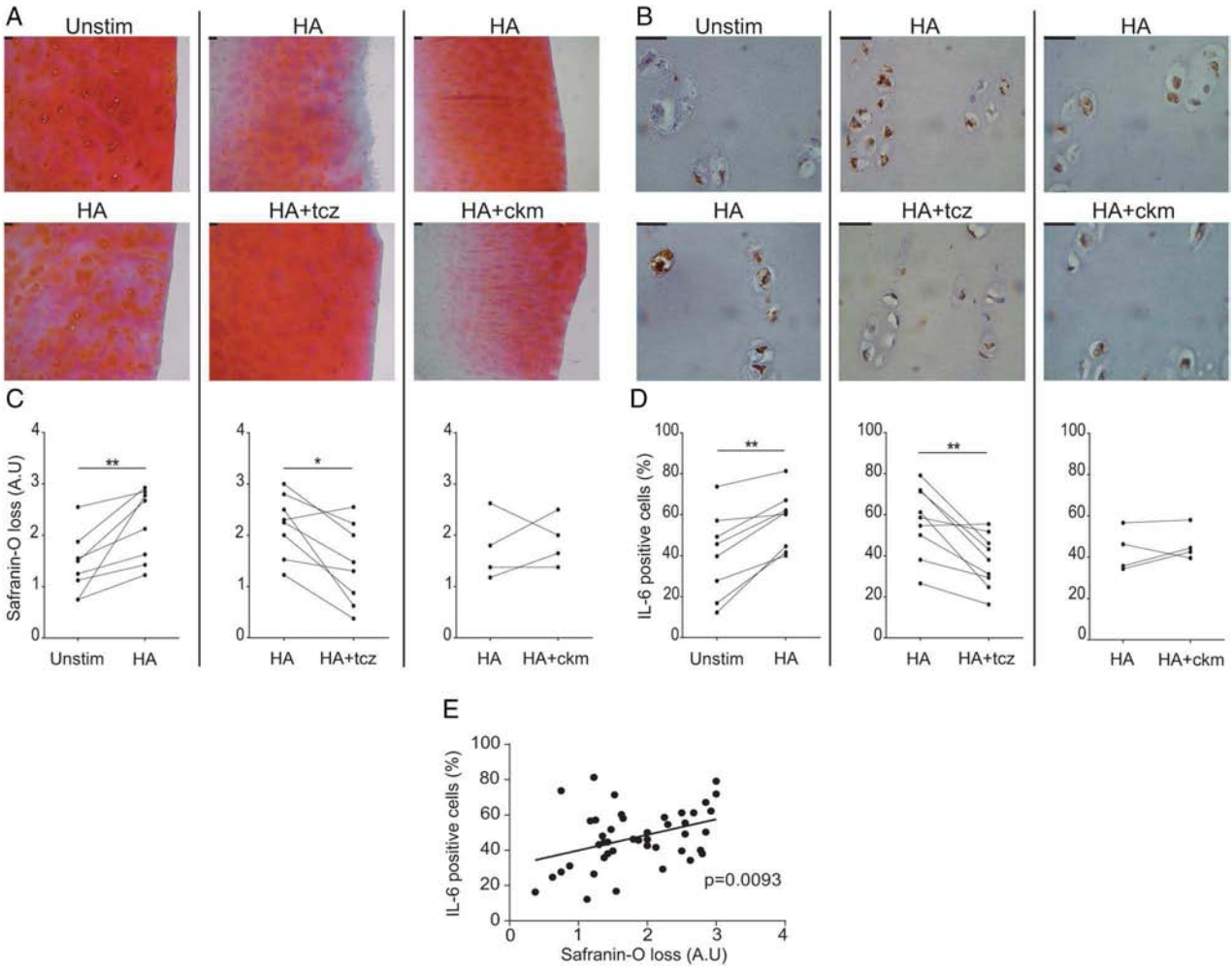

Figure 2 Hydroxyapatite (HA) crystals induce proteoglycan loss and IL-6 production in human cartilage explants. (A and B) Safranin-O staining (A) and IL-6 immunohistochemistry (B) of human cartilage explants stimulated 24 h with HA crystals (HA) or not (Unstim) and treated or not with tocilizumab (tcz) or canakinumab (ckm). Scale bars (50 μm). (C and D) Human cartilage explants Safranin-O loss score (C) and IL-6 positive cells (D) in three independent fields. Matched halves of cartilage tissues are connected by a line (Explants number: 4–8 for each condition). *p<0.05, **p<0.01, ***p<0.001, ****p<0.0001. (E) Correlation graph between IL-6 positive cells and Safranin-O loss in human cartilage explants.

catabolism. Explants were cultured in the presence or absence of HA crystals for 24 h. We observed loss of Safranin-O staining in HA-stimulated explants compared with unstimulated ones (figure 2A, left), confirmed by Safranin-O scoring (figure 2C, left). We next studied the role of IL-6 in HA crystal-induced matrix degradation by adding an IL-6 receptor inhibitor (tocilizumab) to the culture and we observed a significant protection against cartilage degradation as well as matrix degeneration (figure 2A, middle). As a control, we incubated HA-stimulated explants with an anti-IL-1β antibody (canakinumab). This isotype-matched control antibody had no effect on proteoglycan depletion (figure 2A, right). Safranin-O scoring confirmed the protective effect of IL-6 blockade and no effect of IL-1β inhibition (figure 2C middle and right). These results strongly suggested that IL-6 is involved in cartilage degradation.

We also checked if HA crystals induced IL-6 in explants. HA crystals increased chondrocyte IL-6 staining in the transitional zone of cartilage, where pictures were taken (figure 2B, D left). This was inhibited by tocilizumab, but not by canakinumab (figure 2B, D middle and right). Finally, as in the murine model, we found a positive correlation between Safranin-O loss and IL-6 expression (figure 2E). The importance of IL-6 in cartilage matrix degradation is further strengthened by the finding that when HA crystals were added to cartilage explants, we failed to detect any secreted IL-1β or TNF-α but just IL-6, as we previously found in murine chondrocytes. Second, HA-mediated IL-6 release was reduced in explants exposed to IL-6 pathway blockade but not by IL-1β inhibition (results not shown). Taken together, these findings strongly suggest that HA-induced cartilage degradation is IL-6 dependent.

IL-6 increases BCP formation by chondrocytes

As cartilage IL-6 secretion correlated with matrix degradation, and was induced by BCP crystals, we investigated if IL-6, in turn, could induce calcium-containing crystal formation in chondrocyte cultures. After 7 days of culture, Alizarin red staining (figure 3A, black arrows) in IL-6-stimulated chondrocytes was significantly increased compared with unstimulated cells. This was confirmed by spectrophotometric quantification of Alizarin red, after acidic extraction of crystals from the entire cell monolayer (figure 3B). Interestingly, IL-6-induced crystal formation was abrogated by the addition of piceatannol,

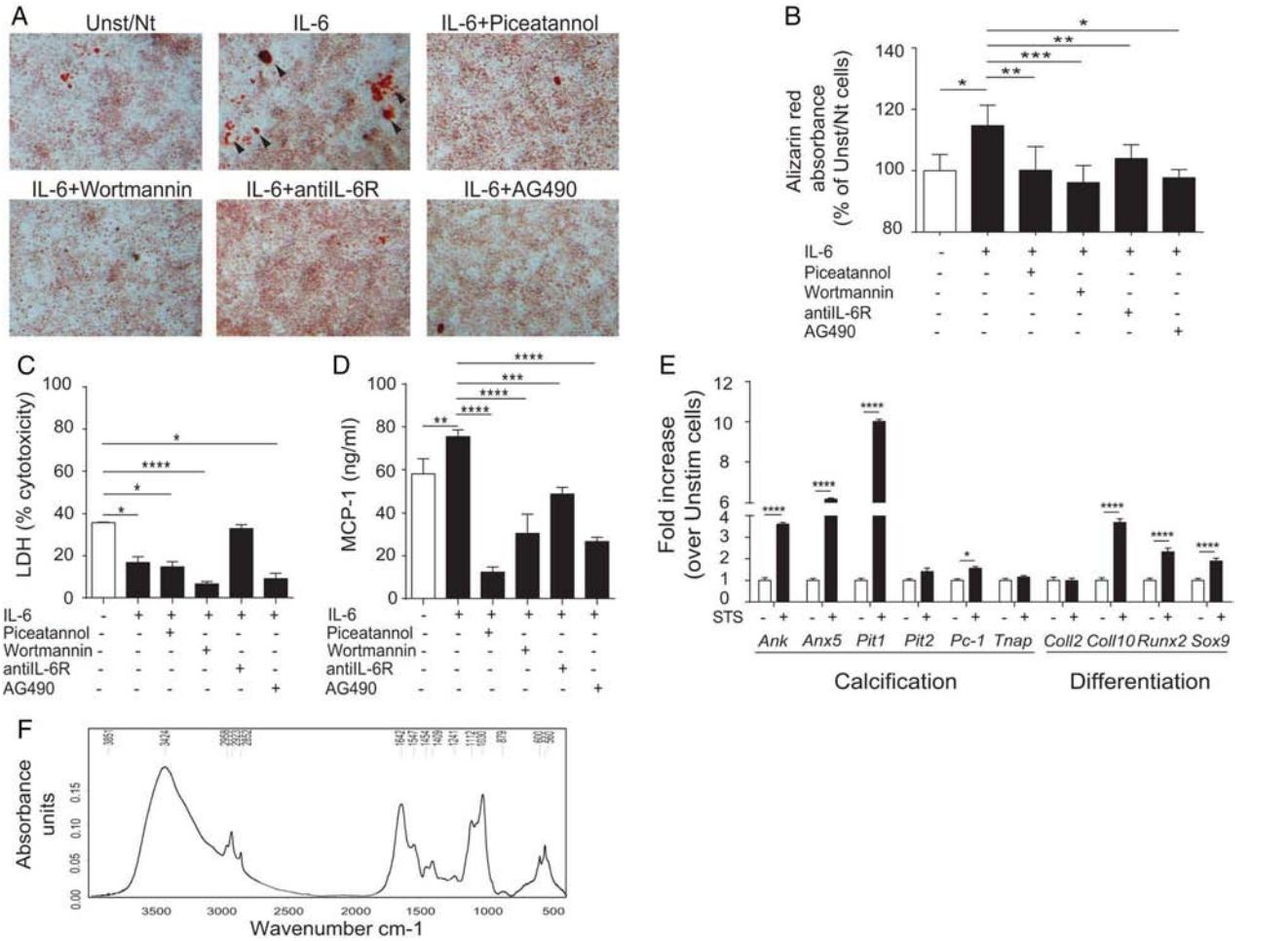

Figure 3 IL-6 induces crystal deposits and MCP-1 secretion in chondrocytes, both blocked by IL-6 inhibitors. (A) Alizarin red staining, (B) Alizarin red absorbance at 405 nm, (C) LDH release and (D) MCP-1 secretion of murine chondrocytes stimulated or not with IL-6 and treated or not with piceatannol (100 μM), Wortmannin (20 μM), anti-IL6R (8 μg/mL) and AG490 (50 μM) for 7 days. Pictures are representative of triplicates of one representative experiment. Values represent means±SD of triplicates from one representative experiment. (E) qRT-PCR of the indicated genes in murine chondrocytes treated or not with IL-6 for 4 h. Values represent means±SD of triplicate samples from one representative experiment. *p<0.05, **p<0.01, ***p<0.001, ****p<0.0001. (F) Biochemical composition of calcium-containing crystals in IL-6 stimulated chondrocytes was assessed by fourier-transform infrared spectroscopy, displaying a characteristic spectrum of octacalcium phosphate crystals (as shown by the phosphate bands at 1112/cm and 1030/cm and phosphate deformation at 600/cm and 560/cm).

Wortmannin, an anti-IL-6R antibody and AG490 (figure 3A, B), the same inhibitors that were able to decrease BCP crystal-induced IL-6 secretion. These inhibitory effects could not be attributed to cytotoxic effects as lactate dehydrogenase (LDH) activity was similar or lower to controls for all the tested inhibitors (figure 3C).

FTIR analysis of the calcium-containing crystals produced by IL-6-stimulated chondrocytes showed the presence of BCP crystals, specifically OCP crystals (phosphate bands at 1112/cm and 1030/cm and phosphate deformation at 600/cm and 560/cm) (figure 3F). In addition to Alizarin red staining, as a control of IL-6 biological activity, we measured MCP-1 secretion, known to be induced by IL-6. Its secretion was increased by IL-6 and significantly decreased by the different inhibitors (figure 3D).

Finally, we investigated the underlying mechanism by which IL-6 promotes calcium-containing crystal formation in chondrocytes by qRT-PCR (figure 3E). IL-6 was able to upregulate the expression of three genes involved in the calcification process (*Ank*, *Anx5* and *Pit-1*). No modulation was detected for genes codifying for other proteins involved in crystal formation (*Pit-2*, *Pc-1* and *Tnap*). Furthermore, IL-6 increased *Coll10* and *Runx2*, markers of hypertrophic chondrocytes, and *Sox9*, marker of early chondrocytic differentiation. Therefore, IL-6 effect on mineralisation cannot simply be explained in terms of impact on the global chondrocytic differentiation.

DISCUSSION

What links biomechanical stress and inflammatory responses to cartilage breakdown in OA is not clearly understood, but there is persuasive evidence that calcification of joint structures could be involved. We demonstrated that in the murine meniscectomy model of OA, calcium-containing crystal deposits were formed in the articular space prior to cartilage degradation (see online supplementary figure S1). These crystal deposits were previously identified as hypertrophic calcification,[36] ectopic bone,[37] mineralised area[38] and heterotopic cartilage,[39] but their chemical characterisation and their role in OA had never been determined. Starting from 1 month after OA induction, microCT-scan revealed multiple deposits within the joint, detached from bone, so that they could not be considered as osteophytes. These structures were composed of bone-like and cartilage-like tissues, showed catabolic and anabolic features typical of OA cartilage[40] and contained CA crystals (see online supplementary figure S2). These structures resembled human synovial osteochondromatosis, a condition associated with OA,[41–43] characterised by chondroid metaplasia and

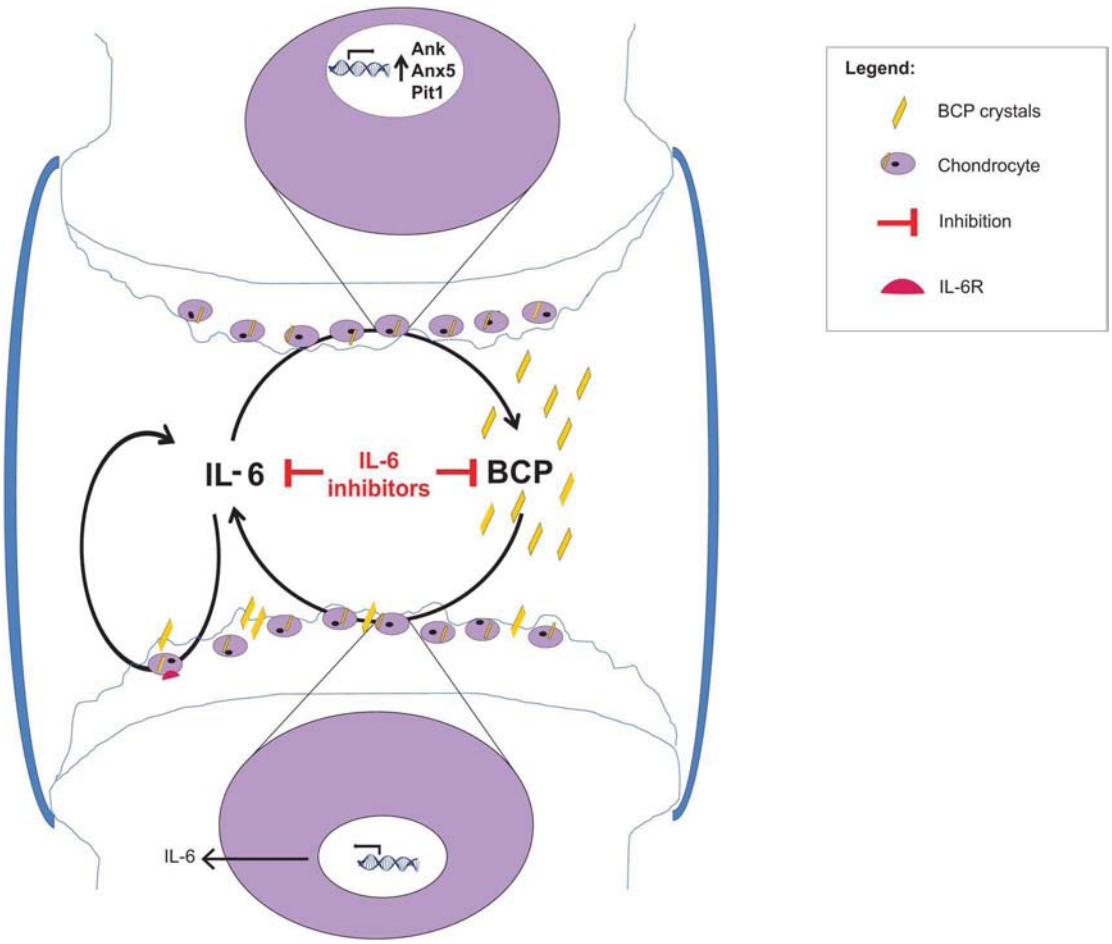

Figure 4 Proposed mechanism based on the obtained results. In osteoarthritis (OA) joints, there is increased basic calcium phosphate (BCP) crystal deposition. These crystals stimulate IL-6 synthesis by articular chondrocytes. IL-6 in turn stimulates IL-6 production in an autocrine way and crystal deposition by inducing genes for calcification: *Ank*, *Anx5* and *Pit1*. This would lead to sustain BCP crystal-induced IL-6 production. IL-6 and BCP crystals induce cartilage matrix-degrading enzymes (such as Mmp-3 and Mmp-13 and Adamts-4 and Adamts-5) in chondrocytes, and subsequent cartilage degradation. This vicious circle suggests that OA can be classified as an autoinflammatory disease. Blocking this circle by an inhibitor of IL-6 will hence reduce IL-6 secretion, chondrocyte crystal formation and cartilage damage.

osteocartilaginous mineralised bodies in the capsule. A process similar to chondroid metaplasia may be involved, whereby fibroblasts undergo metaplastic transformation to chondrocytes, which then calcify.

Calcium phosphate crystals can have multiple effects on chondrocytes, including iNOS gene expression, NO production,[20] Mmp-13 induction,[22] intracellular calcium oscillations[44] and apoptosis.[45] We show here that BCP crystals (in the form of HA) additionally induced *Mmp-3*, *Adamts-4* and *Adamts-5* expression in chondrocytes. Moreover, these microcrystals strongly upregulated IL-6 at the transcriptional and translational levels, while IL-1α, IL-1β and TNF-α cytokines remained undetectable.

We suggest that IL-6 secretion upon crystal stimulation is a result of IL-6 directly induced by BCP (direct pathway) plus IL-6 induced via ligation to its IL-6R, expressed on chondrocytes[27 46] (autocrine pathway). We further found that pharmacological inhibition of the kinases Syk and PI3 and of the signalling molecules Jak2 and Stat3 completely abrogated BCP-induced IL-6 secretion, suggesting that these molecules are implicated in the IL-6 direct and in the IL-6 autocrine pathways. Interestingly, in the presence of saturating concentrations of the neutralising anti-IL-6R antibody, we observed only partial inhibition of crystal-induced IL-6, whereas complete inhibition occurred with Jak and Stat inhibitors. This latter result suggests that IL6-independent, but Jak, Stat-dependent pathways induced by other gp130 signalling cytokines such as Oncostatin M could be involved.[47] We then analysed the consequences of IL-6 blockade in human cartilage explants. HA crystal-stimulated explants showed increased proteoglycan loss and IL-6 expression. Treatment of HA crystal-stimulated explants with an IL-6 inhibitor led to restoration of proteoglycan synthesis and IL-6 expression. These findings suggest that chondrocytes secrete IL-6 that, in turn, binds to its receptor resulting in an autocrine loop. In contrast, addition of an isotype matched IL-1β inhibitor blocking antibody did not exert any protective role with respect to HA crystal-induced proteoglycan loss and IL-6 expression.

IL-1β and TNF-α cytokines, as in BCP-stimulated chondrocytes, remained undetectable. Although IL-1 has been proposed to be a key catabolic cytokine in OA,[48] we were unable to confirm its importance in our previous and current studies. Mice deficient for IL-1α, IL-1β and the adaptor molecule MyD88 were not protected from experimental OA (Nasi *et al*[29] in preparation). These experiments suggest that IL-1β might not be involved in OA pathogenesis whereas IL-6 could be a key cytokine in cartilage degradation induced by crystal stress.

To further support a key role of IL-6 in OA pathogenesis, we have shown here that IL-6 is able to enhance in vitro BCP crystal formation by primary murine chondrocytes and that, indeed, IL-6 inhibitors block in vitro crystal generation. It is interesting to note that OCP crystals, considered a precursor phase of apatite crystals and representing a recent mineralisation process, were the only crystals detected in our chondrocytes after 1 week cell culture. Later on, OCP crystals are normally converted to apatite (CA) crystals, which are indeed the crystals we found in our crystal deposits 2 months after meniscectomy in the in vivo experiments The promineralisation effect of IL-6 cannot simply result from IL-6-effects on chondrocyte differentiation as IL-6 increased *Coll10* and *Runx2*, two markers of hypertrophic chondrocytes, and *Sox9*, an early chondrocytic differentiation marker. We next hypothesise IL-6 may directly modulate one or several of the crucial proteins involved in chondrocyte mineralisation. Indeed, IL-6 was able to upregulate *Ank*, *Anx5* and *Pit-1* gene expression. Ank increases ePPi (that can be hydrolysed in Pi by Tnap) whereas Anx5 and Pit1 concentrate Ca2+ and Pi, respectively, into matrix vesicles and overexpression of Ank, or Anx5, or Pit1 was shown to induce BCP crystal formation.[49–51] Therefore IL-6 upregulation of Ank, or Anx5, or Pit1 genes could act in concert to promote BCP crystal formation in chondrocytes. Whether IL-6 inhibitors block calcification through direct modulation of these genes involved in calcification remains to be clarified.

In conclusion, our results strongly suggest that BCP crystal-induced stress and IL-6 production are interlinked key factors in OA pathogenesis (figure 4). Therefore, inhibition of calcification or of IL-6 signalling pathway represents possible therapeutic approaches for OA treatment.

Acknowledgements The authors thank Professor Frédéric Lioté and Dr Hang-Korng Ea (Hospital Lariboisière and Uniersité Paris Diderot, UFR de Médecine) for helpful discussions, Véronique Chobaz (Laboratory of Rheumatology, CHUV, Lausanne-CH) for her excellent technical support, Prof Brigitte Haeberli-Jolles (DAL, CHUV, Lausanne-CH) for kindly providing human cartilage, Dr Florence Morgenthaler (CIF, University of Lausanne-CH) for her constant support in micro CT-scan analysis and Dr Kempf and Dr Bianchi (CNRS-Université de Lorraine, Nancy, France) for Ank experiments. The authors also thank Dr Peter van Lent (University of Nijmegen, The Netherlands) for his generous help with the anti-VDIPEN staining experiment.

Contributors SN, AS and NB designed, performed and evaluated all experiments. CC synthesised calcium-containing crystals; MD performed FTIR analysis; the entire work was supervised by NB. The figures were prepared and the manuscript was written by SN, AS and NB. All authors discussed and commented on the manuscript.

Funding This work was supported by the Fonds National Suisse de la recherche scientifique (grant 310030-130085/1 and 310030-153010/1), the Institute of Arthritis Research, the Fondation RMR, the Fondation Jean and Linette Warnery.

Competing interests None declared.

Patient consent Obtained.

Ethics approval CHUV Ethical Committee.

Provenance and peer review Not commissioned; externally peer reviewed.

REFERENCES

1 Loeser RF, Goldring SR, Scanzello CR, *et al*. Osteoarthritis: a disease of the joint as an organ. *Arthritis Rheum* 2012;64:1697–707.
2 Nalbant S, Martinez JA, Kitumnuaypong T, *et al*. Synovial fluid features and their relations to osteoarthritis severity: new findings from sequential studies. *Osteoarthritis Cartilage* 2003;11:50–4.
3 Fuerst M, Bertrand J, Lammers L, *et al*. Calcification of articular cartilage in human osteoarthritis. *Arthritis Rheum* 2009;60:2694–703.
4 Fuerst M, Niggemeyer O, Lammers L, *et al*. Articular cartilage mineralization in osteoarthritis of the hip. *BMC Musculoskelet Disord* 2009;10:166.
5 Scotchford CA, Greenwald S, Ali SY. Calcium phosphate crystal distribution in the superficial zone of human femoral head articular cartilage. *J Anat* 1992;181(Pt 2):293–300.
6 Mitsuyama H, Healey RM, Terkeltaub RA, *et al*. Calcification of human articular knee cartilage is primarily an effect of aging rather than osteoarthritis. *Osteoarthritis Cartilage* 2007;15:559–65.
7 Ea HK, Liote F. Advances in understanding calcium-containing crystal disease. *Curr Opin Rheumatol* 2009;21:150–7.
8 Liote F, Ea HK. Clinical implications of pathogenic calcium crystals. *Curr Opin Rheumatol* 2014;26:192–6.
9 Ea HK, Nguyen C, Bazin D, *et al*. Articular cartilage calcification in osteoarthritis: insights into crystal-induced stress. *Arthritis Rheum* 2011;63:10–18.
10 Gurley KA, Reimer RJ, Kingsley DM. Biochemical and genetic analysis of ANK in arthritis and bone disease. *Am J Hum Genet* 2006;79:1017–29.
11 Gurley KA, Chen H, Guenther C, *et al*. Mineral formation in joints caused by complete or joint-specific loss of ANK function. *J Bone Miner Res* 2006;21:1238–47.
12 Bertrand J, Nitschke Y, Fuerst M, *et al*. Decreased levels of nucleotide pyrophosphatase phosphodiesterase 1 are associated with cartilage calcification in osteoarthritis and trigger osteoarthritic changes in mice. *Ann Rheum Dis* 2012;71:1249–53.
13 Sun Y, Mauerhan DR, Honeycutt PR, *et al*. Calcium deposition in osteoarthritic meniscus and meniscal cell culture. *Arthritis Res Ther* 2010;12:R56.
14 Ea HK, Chobaz V, Nguyen C, *et al*. Pathogenic role of basic calcium phosphate crystals in destructive arthropathies. *PLoS ONE* 2013;8:e57352.
15 McCarthy GM, Augustine JA, Baldwin AS, *et al*. Molecular mechanism of basic calcium phosphate crystal-induced activation of human fibroblasts. Role of nuclear factor kappab, activator protein 1, and protein kinase c. *J Biol Chem* 1998;273:35161–9.

16 Nair D, Misra RP, Sallis JD, *et al*. Phosphocitrate inhibits a basic calcium phosphate and calcium pyrophosphate dihydrate crystal-induced mitogen-activated protein kinase cascade signal transduction pathway. *J Biol Chem* 1997;272:18920–5.
17 Brogley MA, Cruz M, Cheung HS. Basic calcium phosphate crystal induction of collagenase 1 and stromelysin expression is dependent on a p42/44 mitogen-activated protein kinase signal transduction pathway. *J Cell Physiol* 1999;180:215–24.
18 Sun Y, Wenger L, Brinckerhoff CE, *et al*. Basic calcium phosphate crystals induce matrix metalloproteinase-1 through the Ras/mitogen-activated protein kinase/c-Fos/AP-1/metalloproteinase 1 pathway. Involvement of transcription factor binding sites AP-1 and PEA-3. *J Biol Chem* 2002;277:1544–52.
19 Reuben PM, Sun Y, Cheung HS. Basic calcium phosphate crystals activate p44/42 MAPK signal transduction pathway via protein kinase Cmicro in human fibroblasts. *J Biol Chem* 2004;279:35719–25.
20 Ea HK, Uzan B, Rey C, *et al*. Octacalcium phosphate crystals directly stimulate expression of inducible nitric oxide synthase through p38 and JNK mitogen-activated protein kinases in articular chondrocytes. *Arthritis Res Ther* 2005;7:R915–926.
21 Cunningham CC, Mills E, Mielke LA, *et al*. Osteoarthritis-associated basic calcium phosphate crystals induce pro-inflammatory cytokines and damage-associated molecules via activation of Syk and PI3 kinase. *Clin Immunol* 2012;144:228–36.
22 McCarthy GM, Westfall PR, Masuda I, *et al*. Basic calcium phosphate crystals activate human osteoarthritic synovial fibroblasts and induce matrix metalloproteinase-13 (collagenase-3) in adult porcine articular chondrocytes. *Ann Rheum Dis* 2001;60:399–406.
23 Livshits G, Zhai G, Hart DJ, *et al*. Interleukin-6 is a significant predictor of radiographic knee osteoarthritis: the Chingford Study. *Arthritis Rheum* 2009;60:2037–45.
24 Hashizume M, Mihara M. Desirable effect of combination therapy with high molecular weight hyaluronate and NSAIDs on MMP production. *Osteoarthritis Cartilage* 2009;17:1513–18.
25 Suzuki M, Hashizume M, Yoshida H, *et al*. IL-6 and IL-1 synergistically enhanced the production of MMPs from synovial cells by up-regulating IL-6 production and IL-1 receptor I expression. *Cytokine* 2010;51:178–83.
26 Sui Y, Lee JH, DiMicco MA, *et al*. Mechanical injury potentiates proteoglycan catabolism induced by interleukin-6 with soluble interleukin-6 receptor and tumor necrosis factor alpha in immature bovine and adult human articular cartilage. *Arthritis Rheum* 2009;60:2985–96.
27 Ryu JH, Yang S, Shin Y, *et al*. Interleukin-6 plays an essential role in hypoxia-inducible factor 2alpha-induced experimental osteoarthritic cartilage destruction in mice. *Arthritis Rheum* 2011;63:2732–43.
28 Kamekura S, Hoshi K, Shimoaka T, *et al*. Osteoarthritis development in novel experimental mouse models induced by knee joint instability. *Osteoarthritis Cartilage* 2005;13:632–41.
29 Nasi S, Ea HK, Chobaz V, *et al*. Dispensable role of myeloid differentiation primary response gene 88 (MyD88) and MyD88-dependent toll-like receptors (TLRs) in a murine model of osteoarthritis. *Joint Bone Spine* 2014;81:320–4.
30 van Lent PL, Grevers LC, Blom AB, *et al*. Stimulation of chondrocyte-mediated cartilage destruction by S100A8 in experimental murine arthritis. *Arthritis Rheum* 2008;58:3776–87.
31 Prudhommeaux F, Schiltz C, Liote F, *et al*. Variation in the inflammatory properties of basic calcium phosphate crystals according to crystal type. *Arthritis Rheum* 1996;39:1319–26.
32 Gosset M, Berenbaum F, Thirion S, *et al*. Primary culture and phenotyping of murine chondrocytes. *Nat Protoc* 2008;3:1253–60.
33 Estepa-Maurice L, Hennequin C, Marfisi C, *et al*. Fourier transform infrared microscopy identification of crystal deposits in tissues: clinical importance in various pathologies. *Am J Clin Pathol* 1996;105:576–82.
34 Nguyen C, Ea HK, Thiaudiere D, *et al*. Calcifications in human osteoarthritic articular cartilage: ex vivo assessment of calcium compounds using XANES spectroscopy. *J Synchrotron Radiat* 2011;18:475–80.
35 Gregory CA, Gunn WG, Peister A, *et al*. An Alizarin red-based assay of mineralization by adherent cells in culture: comparison with cetylpyridinium chloride extraction. *Anal Biochem* 2004;329:77–84.
36 Tremoleda JL, Khalil M, Gompels LL, *et al*. Imaging technologies for preclinical models of bone and joint disorders. *EJNMMI Res* 2011;1:11.
37 Glasson SS, Blanchet TJ, Morris EA. The surgical destabilization of the medial meniscus (DMM) model of osteoarthritis in the 129/SvEv mouse. *Osteoarthritis Cartilage* 2007;15:1061–9.
38 Sampson ER, Beck CA, Ketz J, *et al*. Establishment of an index with increased sensitivity for assessing murine arthritis. *J Orthop Res* 2011;29:1145–51.
39 Aini H, Ochi H, Iwata M, *et al*. Procyanidin B3 prevents articular cartilage degeneration and heterotopic cartilage formation in a mouse surgical osteoarthritis model. *PLoS ONE* 2012;7:e37728.
40 Mueller MB, Tuan RS. Anabolic/Catabolic balance in pathogenesis of osteoarthritis: identifying molecular targets. *PM R* 2011;3:S3–11.
41 Fuerst M, Zustin J, Lohmann C, *et al*. [Synovial chondromatosis]. *Orthopade* 2009;38:511–19.
42 Fukui K, Kaneuji A, Amaya S, *et al*. Synovial osteochondromatosis of the hip with femoroacetabular impingement and osteoarthritis: a case report. *J Orthop Surg (Hong Kong)* 2013;21:117–21.
43 Ladefoged C. Amyloid in osteoarthritic hip joints: deposits in relation to chondromatosis, pyrophosphate, and inflammatory cell infiltrate in the synovial membrane and fibrous capsule. *Ann Rheum Dis* 1983;42:659–64.
44 Nguyen C, Lieberherr M, Bordat C, *et al*. Intracellular calcium oscillations in articular chondrocytes induced by basic calcium phosphate crystals lead to cartilage degradation. *Osteoarthritis Cartilage* 2012;20:1399–408.
45 Ea HK, Monceau V, Camors E, *et al*. Annexin 5 overexpression increased articular chondrocyte apoptosis induced by basic calcium phosphate crystals. *Ann Rheum Dis* 2008;67:1617–25.
46 Poree B, Kypriotou M, Chadjichristos C, *et al*. Interleukin-6 (IL-6) and/or soluble IL-6 receptor down-regulation of human type II collagen gene expression in articular chondrocytes requires a decrease of Sp1.Sp3 ratio and of the binding activity of both factors to the COL2A1 promoter. *J Biol Chem* 2008;283:4850–65.
47 Van Wagoner NJ, Choi C, Repovic P, *et al*. Oncostatin M regulation of interleukin-6 expression in astrocytes: biphasic regulation involving the mitogen-activated protein kinases ERK1/2 and p38. *J Neurochem* 2000;75:563–75.
48 Pelletier JP, Caron JP, Evans C, *et al*. In vivo suppression of early experimental osteoarthritis by interleukin-1 receptor antagonist using gene therapy. *Arthritis Rheum* 1997;40:1012–19.
49 Zaka R, Stokes D, Dion AS, *et al*. P5L mutation in Ank results in an increase in extracellular inorganic pyrophosphate during proliferation and nonmineralizing hypertrophy in stably transduced ATDC5 cells. *Arthritis Res Ther* 2006;8:R164.
50 Kirsch T, Swoboda B, Nah H. Activation of annexin II and V expression, terminal differentiation, mineralization and apoptosis in human osteoarthritic cartilage. *Osteoarthritis Cartilage* 2000;8:294–302.
51 Li X, Yang HY, Giachelli CM. Role of the sodium-dependent phosphate cotransporter, Pit-1, in vascular smooth muscle cell calcification. *Circ Res* 2006;98:905–12.